

On the Origin of Stars in Bulges and Elliptical Galaxies

S. Khochfar,^{1*} J. Silk,¹

¹ *Department of Physics, Denys Wilkinson Building, Keble Road, Oxford OX1 3RH, United Kingdom*

Released 2005 Xxxxx XX

ABSTRACT

We investigate the stellar composition of bulges and elliptical galaxies as predicted by the CDM paradigm using semi-analytical modelling. We argue that spheroid stars are built up of two main components, *merger* and *quiescent*, according to the origin of the stars. The merger component is formed during major mergers by gas driven to the centre, while the quiescent component is formed in gaseous discs and added later to the spheroid during major mergers. Galaxies more massive than $M_C = 3 \times 10^{10} M_\odot$ have on average only a 15% merger component in their spheroids, while smaller galaxies can have up to 30%. The merger component increases with redshift due to mergers involving more gas. However we do not find mergers with gas fraction above $\sim 40\%$ of the remnants mass. Generally the gas fraction is a decreasing function of the redshift at which the merger occurs and the mass of the remnant, with more massive remnants having smaller gas fraction and hence smaller merger components. This trend is independent of the environment of the galaxy with the only impact of the environment being that galaxies less massive than M_C have slightly larger merger components in dense environments. The fraction of stars in bulges for galaxies more massive than M_C is larger than 50%. We find that the majority of stars in galaxies more massive than M_C reside within bulges and ellipticals independent of redshift and that the fraction increases with redshift. The most massive galaxies at each redshift are elliptical galaxies.

Key words: dark matter – galaxies: ellipticals – galaxies: formation

1 INTRODUCTION

Bright elliptical galaxies are old stellar systems which formed the bulk of their stars at high redshift within a short time scale (e.g. Cimatti et al. 2004; Thomas et al. 2005). However, they are not a coeval family of objects as they for example divide into luminous slow rotating pressure supported ellipticals, called boxy, and fast rotating less luminous ellipticals (e.g. Bender et al. 1993), called disky. Another deviation of elliptical galaxies suggests that they can be divided into core and power-law galaxies according to the steepness of their inner surface brightness profile (e.g. Lauer et al. 1995). Furthermore, 2-dimensional integral-field spectographs like SAURON or OASIS, reveal kinematically decoupled cores in many elliptical galaxies (e.g. McDermid et al. 2005).

There are two competing scenarios for the formation of elliptical galaxies. One assumes that they are formed at high redshift during a highly efficient starburst followed by passive evolution of the stellar component (e.g. Larson 1974; Chiosi & Carraro 2002), and the other assumes the forma-

tion of an elliptical galaxy in the merger of two galaxies (e.g. Toomre & Toomre 1972). In this paper, we will test the predictions made by the latter model.

Since the early proposal of Toomre & Toomre (1972) that early type galaxies form as the result of a binary merger between two spiral galaxies, many numerical simulations have been performed and compared to observations (e.g. Barnes & Hernquist 1992; Burkert & Naab 2003, and references therein). The general consensus is that it is possible to generate remnants which agree in their kinematic properties with observed elliptical galaxies. Recent merger simulations use self-consistent cosmological initial condition (Khochfar & Burkert 2006), in simulations with only stars (e.g. Naab & Burkert 2003) and in simulations with gas, star formation and feedback (e.g. Cox et al. 2005). Usually these simulations neglect the past history of a possible progenitor galaxy, with the simulations starting from idealised initial conditions.

Observationally, there is evidence that the initial conditions of merging galaxies cover a wide range, from being ‘dry’ (van Dokkum 2005; Bell et al. 2005) to being ultra-luminous (for a review see Schweizer 2005). It is therefore expected that the stars ending up in a spheroid could not all

* sadeghk@astro.ox.ac.uk

have been formed in the same kind of event, but must have formed in different events which depend on the past history of the merging galaxies. Since merger simulations indicate that violent relaxation is not complete and that the stars manage to remember their initial energy and orbital angular momentum (Barnes 1998), it is necessary to take into account the past history of a galaxy. The main task now is to connect these past histories with the properties of merger remnants.

Large observational studies that collect data from several thousands of galaxies, like the Sloan Digital Sky Survey, reveal that the galaxy population follows remarkable trends: e.g. the surface mass density of galaxies increases with mass until a characteristic mass scale of $M_C = 3 \times 10^{10} M_\odot$ at which it becomes constant (Kauffmann et al. 2003). The constant surface mass density is mainly associated with elliptical galaxies and galaxies having significant bulges. Furthermore, detailed studies of the size distribution of elliptical galaxies reveal that the scatter in sizes of elliptical galaxies of a given mass is log-normal distributed with a scatter which decreases for larger galaxy masses (Shen et al. 2003). Those authors could explain the evolution of the sizes by assuming continued mergers of galaxies which had initially all the same mass but sizes that followed an appropriate distribution. The origin of this distribution however remains unsolved. Another interesting observed correlation is that the surface mass density of galaxies in different environments only differs at low masses (Kauffmann et al. 2004).

In this paper, we address the question of where stars that end up in spheroids were formed. The paper is structured as follows: we begin by explaining the model ingredients we use, followed by a section on the past merging history of galaxies. Then we introduce our definition of the two stellar components found in spheroids and discuss how these components evolve in the simulated galaxy population. In section five we present our conclusions.

2 GALAXY FORMATION MODELLING

The main strategy behind the modelling approach we follow is first to calculate the collapse and merging history of individual dark matter halos, which is governed purely by gravitational interactions, and secondly to calculate the more complex physics of the baryons inside these dark matter halos, including e.g. radiative cooling of the gas, star formation, and feedback from supernovae by simplified prescriptions on top of the dark matter evolution. Each of the dark matter halos will consist of three main components which are distributed among individual galaxies inside them: a stellar, cold, and hot gas component, where the latter is only attributed to *central* galaxies, which are the most massive galaxies inside individual halos. In the following sections, we will describe briefly the recipes used to calculate these different components which are mainly based on recipes presented in e.g. Cole et al. (1994, 2000), Kauffmann et al. (1999) (hereafter, K99) and Springel et al. (2001) (hereafter, S01), and we refer readers for more details on model implementations to their work and references therein.

Throughout this paper we use the following set of cosmological parameters: $\Omega_0 = 0.3$, $\Omega_\Lambda = 0.7$, $\Omega_b/\Omega_0 = 0.15$, $\sigma_8 = 0.9$ and $h = 0.65$.

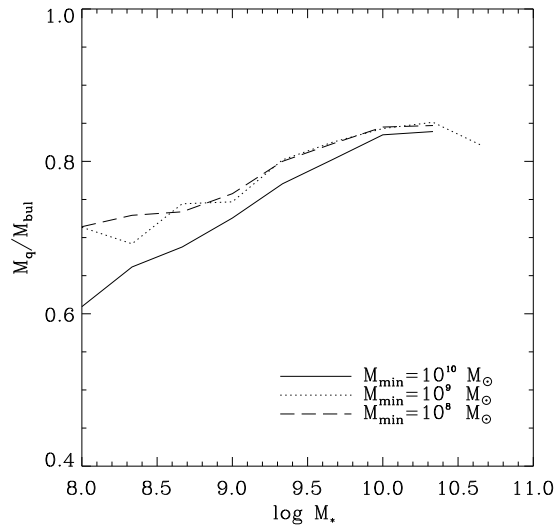


Figure 1. Average mass fraction of disc stars populating spheroids depending on the mass resolution M_{min} of the merger tree.

2.1 Dark Matter Evolution

We calculate the merging history of dark matter halos according to the prescription presented in Somerville & Kolatt (1999a). This approach has been shown to produce merging histories and progenitor distributions in reasonable agreement with results from N-body simulations of cold dark matter structure formation in a cosmological context (Somerville et al. 2000). The merging history of dark matter halos is reconstructed by breaking each halo up into progenitors above a limiting minimum progenitor mass M_{min} . This mass cut needs to be chosen carefully as it ensures that the right galaxy population and merging histories are produced within the model. Progenitor halos with masses below M_{min} are declared as *accretion* events and their histories are not followed further back in time. Progenitors labelled as accretion events should ideally not host any significant galaxies in them and be composed mainly of primordial hot gas at the progenitor halo's virial temperature. The mass scale at which this is the case can in principle be estimated from the prescriptions of supernova feedback and reionization presented in section 2.2.1. However, to achieve a good compromise between accuracy and computational time, we instead estimated M_{min} by running several simulations with different resolutions and chose the resolution for which results in the galaxy mass range of interest are independent of the specific choice of M_{min} . Changing the mass resolution mainly affects our results at low galaxy mass scales as shown in Fig.1, leaving massive galaxies nearly unaffected. Throughout this paper we will use $M_{min} = 2 \times 10^9 M_\odot$ which produces numerically stable results for galaxies with stellar masses $M_* \geq 10^9 M_\odot$.

2.2 Baryonic Physics

As mentioned above, once the merging history of the dark matter component has been calculated, it is possible to fol-

low the evolution of the baryonic content in these halos forward in time. We assume each halo consists of three components: hot gas, cold gas and stars, where the latter two components can be distributed among individual galaxies inside a single dark matter halo. The stellar components of each galaxy are additionally divided into bulge and disc, to allow morphological classifications of model galaxies. In the following, we describe how the evolution of each component is calculated.

2.2.1 Gas Cooling & Reionization

Each branch of the merger tree starts at a progenitor mass of M_{min} and ends at a redshift of $z = 0$. Initially, each halo is occupied by hot primordial gas which was captured in the potential well of the halo and shock heated to its virial temperature $T_{vir} = 35.9 [V_c / (\text{km s}^{-1})]^2 \text{ K}$, where V_c is the circular velocity of the halo (White & Frenk 1991, K99). Subsequently this hot gas component is allowed to radiatively cool and settles down into a rotationally supported gas disc at the centre of the halo, which we identify as the central galaxy (e.g. Silk 1977; White & Rees 1978; White & Frenk 1991). The rate at which hot gas cools down is estimated by calculating the cooling radius inside the halo using the cooling functions provided by Sutherland & Dopita (1993) and the prescription in S01. In the case of a merger between halos we assume that all of the hot gas present in the progenitors gets shock heated to the virial temperature of the remnant halo, and that gas can only cool down onto the new central galaxy which is the central galaxy of the most massive progenitor halo. The central galaxy of the less massive halo will become a satellite galaxy orbiting inside the remnant halo. In this way, a halo can host multiple satellite galaxies, depending on the merging history of the halo, but will always only host one central galaxy onto which gas can cool. The cold gas content in satellite galaxies is given by the amount present when they first became satellite galaxies and does not increase, instead it decreases due to ongoing star formation and supernova feedback.

In the simplified picture adopted above, the amount of gas available to cool down is only limited by the universal baryon fraction $\Omega_b h^2 = 0.024$ (Spergel et al. 2003). However, in the presence of a photoionising background the fraction of baryons captured in halos is reduced (e.g. Navarro & Steinmetz 1997; Gnedin 2000; Benson et al. 2002) and we use the recipe of Somerville (2002), which is based on a fitting formulae derived from hydrodynamical simulations by Gnedin (2000), to estimate the amount of baryons in each halo. For the epoch of reionisation, we assume $z_{reion} = 20$, which is in agreement with observations of the temperature-polarisation correlation of the cosmic microwave background by Kogut et al. (2003).

2.2.2 Star formation in Discs and Supernova Feedback

Once cooled gas has settled down in a disc, we allow for fragmentation and subsequent star formation according to a parameterised global Schmidt-Kennicutt law (Kennicutt 1998) of the form $\dot{M}_* = \alpha M_{cold} / t_{dyn,gal}$, where α is a free parameter describing the efficiency of the conversion of cold gas into stars, and $t_{dyn,gal}$ is assumed to be the dynamical

time of the galaxy and is approximated to be 0.1 times the dynamical time of the dark matter halo (K99). As in K99 we allow star formation only in halos of $V_c < 350 \text{ km/s}$ to avoid too bright central galaxies in clusters.

Feedback from supernovae plays an important role in regulating star formation in small mass halos and in preventing too massive satellite galaxies from forming. We implement feedback based on the prescription presented in K99 with

$$\Delta M_{reheat} = \frac{4}{3} \epsilon \frac{\eta_{SN} E_{SN}}{V_c^2} \Delta M_*. \quad (1)$$

Here we introduce a second free parameter ϵ which represents our lack of knowledge on the efficiency with which the energy from supernovae is going to reheat the cold gas. The expected number of supernovae per solar mass of stars formed is given by $\eta_{SN} = 5 \times 10^{-3}$, taken as the value for the Scalo initial mass function (Scalo 1986), and $E_{SN} = 10^{51} \text{ erg}$ is the energy output from each supernova. We take V_c as the circular velocity of the halo in which the galaxy was last present as a central galaxy.

2.2.3 Galaxy Mergers

We allow for mergers between galaxies residing in a single halo. As mentioned earlier, each halo is occupied by one central galaxy and a number of satellite galaxies depending on the past merging history of the halo. Whenever two halos merge, the galaxies inside them are going to merge on a time-scale which we calculate by estimating the time it would take the satellite to reach the centre of the halo under the effects of dynamical friction. Satellites are assumed to merge only with central galaxies and we set up their orbits in the halo according to the prescription of K99, modified to use the Coulomb logarithm approximation of S01.

If the mass ratio between the two merging galaxies is $M_{gal,1}/M_{gal,2} \leq 3.5$ ($M_{gal,1} \geq M_{gal,2}$) we declare the event as a *major* merger and the remnant will be an elliptical galaxy and the stellar components and the gas will be treated according to the prescriptions below. In the case of *minor* merger $M_{gal,1}/M_{gal,2} > 3.5$ the cold gas in the disc of the smaller progenitor is assumed to settle down in the gas disc of the remnant and its stars contribute to the bulge component of the remnant (e.g. K99).

2.2.4 Formation of Ellipticals and Bulges

Toomre & Toomre (1972) suggested that major mergers will lead to the formation of elliptical galaxies. Indeed detailed numerical simulations in the last decade seem to support this hypothesis (e.g. Barnes & Hernquist 1992; Burkert & Naab 2003, and reference therein), and we will assume in the following that major mergers disrupt the discs in progenitor galaxies, as seen in various numerical simulations, and relax to a spheroidal distribution. During the merger, any cold gas in the discs of the progenitor galaxies is assumed to be funnelled into the centre of the remnant where it ignites a starburst which transforms all of the cold gas into stars contributing to the spheroidal component (e.g. K99; S01; and references therein). The second assumption is certainly a simplification of what might happen since we neglect the possibility that not all of the cold gas is funnelled to the

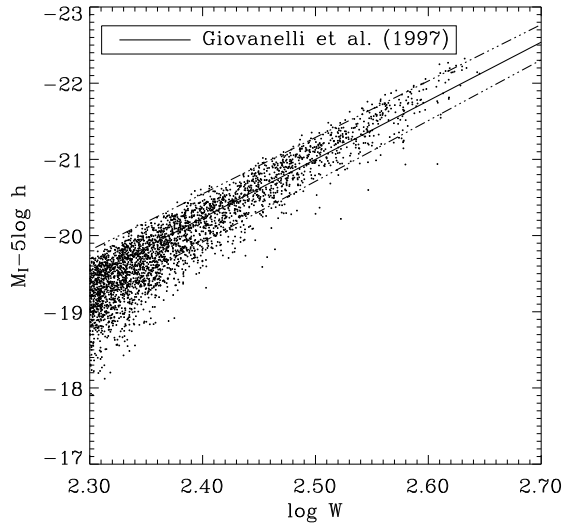


Figure 2. Predicted *I*-band Tully-Fisher relation for Sb/Sc galaxies in our simulation. The solid line is the fit to the observed data by Giovanelli et al. (1997) and dashed lines give their estimate for the scatter.

centre but some fraction of it can e.g. settle down into an extended disk which continues growing inside-out by fresh supply of gas from tidal tails (e.g. Barnes & Hernquist 1991; Mihos & Hernquist 1996; Barnes 2001, 2002). The results of Barnes (2002) indicate that 40% – 80% of the initial gas in the disc could end up in the central region of the remnant and be consumed in a starburst. The exact amount is somewhat dependent on the merger geometry and on the mass ratio of the merger. Unfortunately, a large survey investigating the gas inflow to the centres of merger remnants is not available to date so that we use the simplified approach of assuming that all cold gas gets used up in the central starburst. This prescription for the fate of the cold gas results in an overestimate of the spheroid masses and an underestimate of the secondary disc components in our model. This is not very significant for massive ellipticals since they are mainly formed in relatively weak dissipative mergers (Khochfar & Burkert 2003).

Another simplifying assumption is that we neglect the feeding of super massive black holes in the centre of the remnant or feedback effects on the gas from the central source. However, Haehnelt & Kauffmann (2000) estimate that a cold gas mass fraction of less than 1% accreted onto the black hole is sufficient to recover the $M_{\bullet} - \sigma$ relation and we therefore neglect this effect on the amount of gas available for the central starburst. A larger effect on our results arises from the fact that we neglect feedback from the central source into the surrounding intergalactic medium. As a consequence, our estimates of stars formed in a central starburst will be too high and should be viewed as upper limits.

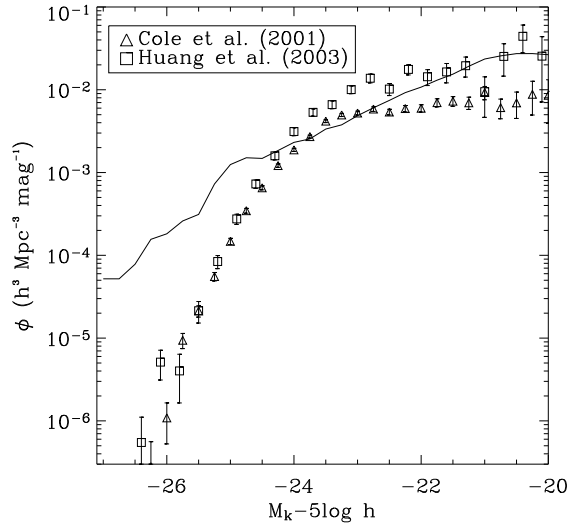


Figure 3. The predicted *K*-band luminosity function in our simulation in comparison to the observations by Cole et al. (2001) and Huang et al. (2003).

2.2.5 Free parameters and predicted present-day properties of modelled galaxies

We normalise our two model parameters for the star formation efficiency α and feedback efficiency ϵ by matching the *I*-band Tully-Fisher relation of Giovanelli et al. (1997) and requiring that spiral central galaxies of halos with circular velocity $V_C = 220$ km/s have on average $10^{11} M_{\odot}$ of stars and a few times $10^9 M_{\odot}$ of cold gas (Somerville & Kolatt 1999b). The best fit model parameters we get in this way are $\epsilon = 0.2$ and $\alpha = 0.1$.

Figure 2 shows our predicted *I*-band Tully-Fisher relation for Sb/Sc galaxies in comparison to the observed one by Giovanelli et al. (1997). We selected Sb/Sc galaxies following Simien & de Vaucouleurs (1986) according to their bulge to total light in the range $1.5 \leq M_{B,bulge} - M_{B,total} \leq 2.2$.

The model predictions for the *K*-band luminosities of the overall galaxy population and the early-type galaxy luminosity are shown in Fig. 4 & refmod2, respectively. We choose early-type galaxies to have bulge to total light ratios with $1 \leq M_{B,bulge} - M_{B,total}$, which includes S0 galaxies according to Simien & de Vaucouleurs (1986). Our luminosity functions somehow over predicts the abundance of very luminous objects, which is a known problem and previously discussed in Benson et al. (2003). The solution to this problem is commonly believed to come from AGN-feedback. Croton et al. (2006) who use semi-analytic modelling based on the same recipes that we do find a luminosity function very similar to ours (see Fig.8 of their paper). However, the inclusion of AGN-feedback in their models reduces the amount of very luminous galaxies and fits the data very well at the high mass end. As for our results presented in this paper the neglect of AGN-feedback results in a few too bright and too massive early-type galaxies as can be seen in Fig. 3. However, these galaxies are rare and extreme cases not considered in our analyses. Our early-type luminosity

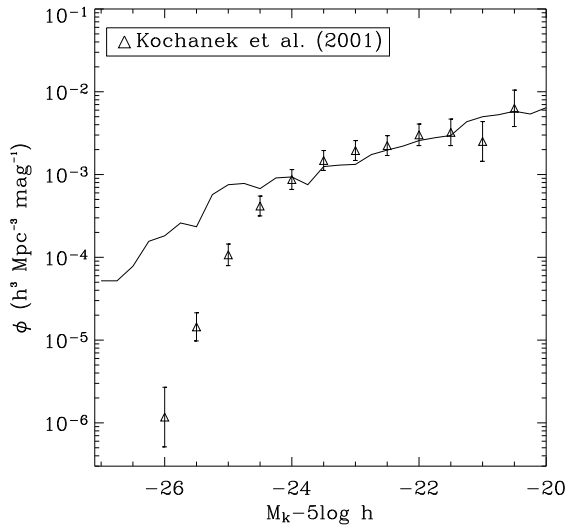


Figure 4. The predicted K -band luminosity function in our simulation for early-type galaxies in comparison to the observations by Kochanek et al. (2001).

fiction fits the data very well over most of the considered range and we therefore delay further discussion of AGN-feedback to a forthcoming paper (Khochfar & Silk in prep.).

3 PAST MERGING HISTORY OF PROGENITOR GALAXIES

The composition of stars in bulges and elliptical galaxies is very dependent on the previous merging history of the progenitors and their ability to cool gas and regrow large stellar discs in between major mergers. Khochfar & Burkert (2003) showed that based on the stellar mass of the remnant, a transition appears at which regrowing of a stellar disc becomes inefficient. This leads to major mergers mainly between bulge-dominated galaxies with too low fractions of available cold gas to ignite central starbursts, sometimes called “dry” mergers. It appears that such a transition is necessary to explain properties like e.g. the isophotal shape of massive elliptical galaxies (Khochfar & Burkert 2005). To stress the importance of taking into account the past merging history of progenitors, we investigate in Fig. 5 the question of the relative number of mergers between galaxies without bulges to the number of mergers between galaxies with bulges, depending on the masses of the remnants. As can be seen, it becomes very unlikely to find mergers between two pure disc galaxies that lead to very massive remnants. At masses above $M_* \simeq 3 \times 10^9 M_\odot$, the majority of mergers take place between galaxies that have already experienced a major merger in their past. It is interesting to note that we do not find any mergers between bulge-less disc galaxies in our simulation at masses larger than the characteristic mass scale M_C , suggesting that the effect of constant surface mass density μ_* in elliptical galaxies more massive than M_C is closely related to the bulge fractions in the progen-

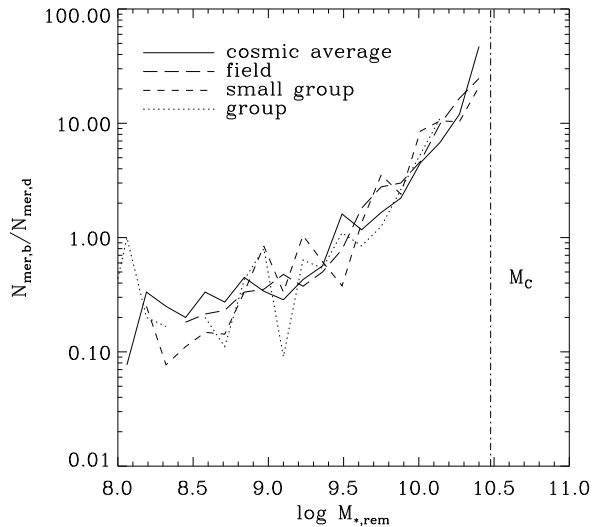


Figure 5. Ratio of the number of mergers between galaxies with bulges and without bulges as a function of the remnant mass found in our simulations. The solid line shows the results for the cosmological mass function of Jenkins et al. (2001), and the other lines examine results for different environments. The vertical dot-dashed line marks the characteristic mass scale $M_C = 3 \times 10^{10} M_\odot$ reported in Kauffmann et al. (2003)

itor galaxies. Inspecting the environmental dependence, we find that the ratios evolve independently of the environment of the galaxy and that bulge-less mergers stop occurring at lower masses in dense environments like groups and clusters. This is a consequence of the higher merger fractions at earlier times in these environments (Khochfar & Burkert 2001).

4 MERGER AND QUIESCENT COMPONENTS IN SPHEROIDS

The populations of stars present in a spheroid at a given time in its evolution are a composite of stars formed in various progenitors at different times and in different modes. Here we distinguish between two modes, the merger-induced ‘merger component’ and the disc mode ‘quiescent component’. The merger component is a composite of all stars that were formed because of the consumption of cold gas during major mergers in progenitor galaxies. On the other hand, the quiescent component is the amount of stars formed in gaseous discs according to the Schmidt-Kennicutt law during the evolution of the progenitor galaxies. When calculating each component for a spheroid, we sum up the mass of the merger component so far and subtract it from the spheroid mass to get the quiescent component.

To investigate systematic trends in the fraction of merger-induced and quiescent stellar components in elliptical galaxies and bulges, we use in the following the conditional distribution

$$p(M_q/M_{bul}|M_*) = \frac{\phi(M_q/M_{bul}, M_*)}{\int \phi(M'_q/M'_{bul}, M_*) d(M'_q/M'_{bul})}, \quad (2)$$

where M_q is the stellar mass in the spheroid previously

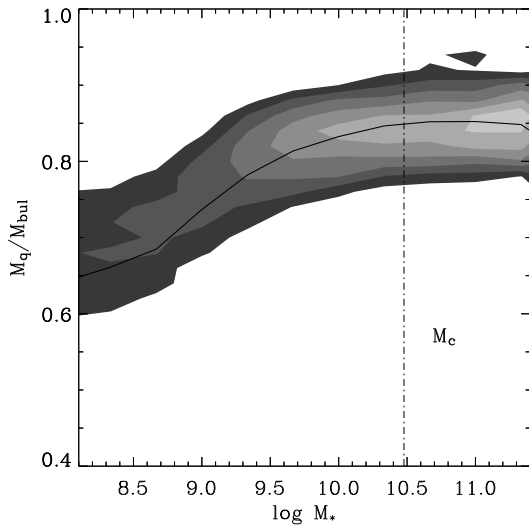


Figure 6. Conditional distribution of the fraction of quiescent stars ending up in spheroids as a function of the total galaxy mass for the overall galaxy population at redshift $z \leq 0.3$. The solid line shows the mean of the distribution and the vertical dot-dashed line marks the characteristic mass scale M_C .

formed quiescently, M_{bul} the mass of the spheroid and M_* the total stellar mass of the galaxy. The merger component in the spheroid is then simply given by $1 - M_q/M_{bul}$. If not stated otherwise, this distribution is derived for the simulated galaxy population at redshifts $z \leq 0.3$.

The quiescent component of stars in spheroids is getting more dominant with galaxy mass up to masses around M_C when it starts becoming a constant fraction of the stars in the spheroid (Fig. 6). The behaviour at galaxy masses below M_C can be understood by acknowledging that massive spheroids form late in the hierarchical galaxy formation paradigm, thereby allowing more stars to be formed in progenitor discs between individual major merger events, and that feedback from supernovae is less efficient in reheating cold gas in discs which are embedded in massive halos. It is worth noting that even spheroids in galaxies as small as $M_* = 10^9 M_\odot$ have on average only $\sim 30\%$ of their stars being formed in past merger-triggered central starbursts, indicating that the main mode of star formation is taking place in discs. The quiescent fraction of stars can get as large as $\sim 85\%$ at masses above M_C , where it then becomes constant.

4.1 Redshift Evolution

The distribution found for the galaxy population at $z \leq 0.3$ is likely to be dependent on redshift. Galaxies at high redshifts tend to have a higher fraction of cold gas available in their discs than their counterparts at low redshift when they participate in mergers as shown in Fig. 9. This is mainly due to the time available to make stars in the disc before the major merger and the very short cooling times for the hot gas. To investigate the build up of the distribution at low redshift, we look at the trajectory of a galaxy defined by its positions in the $M_q/M_{bul} - M_*$ plane through time. Since

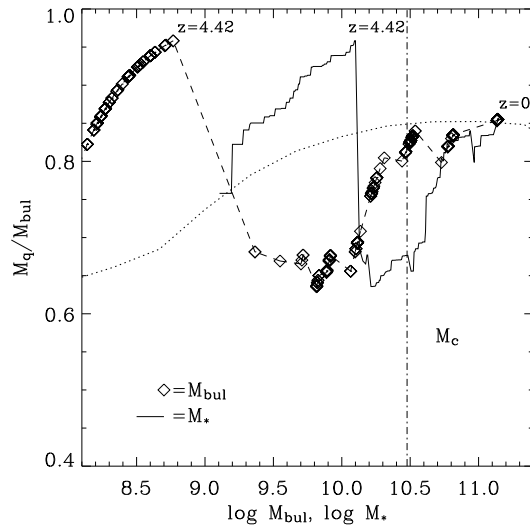


Figure 7. Trajectory of a representative galaxy with final mass $M_* = 1.5 \times 10^{11} M_\odot$ at $z = 0$. We show the evolution as a function of the bulge mass M_{bul} and as a function of the total stellar mass M_* , indicated by the symbols and the solid line, respectively. The average of the overall galaxy distribution is displayed by the dotted line, and the vertical dot-dashed line marks the characteristic mass scale M_C . Please note that the trajectory as a function of total stellar mass starts around $M_* \sim 10^9 M_\odot$ because we start following trajectories after the first occurrence of a major merger between progenitor galaxies. For guidance we label the bulge and total stellar mass at the first occurrence of a significant central star burst with the corresponding redshift of that event ($z = 4.42$) and at a redshift of $z = 0$.

the present day value of M_q is integrated over the entire history of a galaxy, we calculate the trajectories by summing up at each redshift the quiescent stellar components in the individual progenitor bulges and ellipticals and divide it by the sum of the stellar mass of the progenitor spheroids:

$$\frac{M_q(z)}{M_{bul}(z)} = \frac{\sum_{i=1, N_{prog}} M_{q,i}(z)}{\sum_{i=1, N_{prog}} M_{bul,i}(z)}. \quad (3)$$

Note that elliptical galaxies might contain a small disc which is in the process of regrowing, and that we do not attribute these stars to the spheroid when calculating the trajectory. A typical trajectory for an elliptical galaxy more massive than M_C is presented in Fig. 7. This galaxy experienced a gas-rich major merger at a redshift of $z = 4.42$ between two progenitors leading to a significant decrease in the quiescent fraction M_q/M_{bul} . The significant decrease is not only due to the amount of cold gas available in the merger but also to the fact that most of the stars in the individual progenitors are still in their discs, and that only a few, if any, galaxies consist of spheroids, which makes a single major merger have a large impact. Once significant spheroids in the population of progenitors start to exist, major mergers between two progenitors tend to lower the overall fraction of quiescent stellar components only slightly.

The main mode by which M_q/M_{bul} increases is by minor merging with satellite galaxies. These satellite galaxies, though smaller in mass than their central galaxies, have

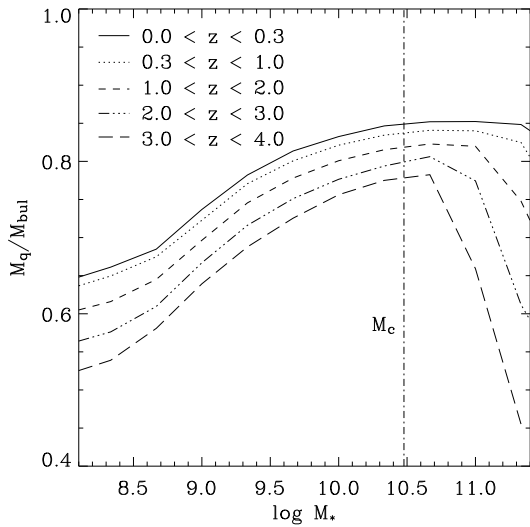


Figure 8. The evolution of the mean value M_q/M_{bul} of the conditional distribution $p(M_q/M_{bul}|M_*)$ as a function of stellar mass M_* in five different redshift bins between $z = 0$ and $z = 4$. The vertical dot-dashed line marks the characteristic mass scale M_C .

grown stellar discs which are massive enough to increase M_q/M_{bul} . That minor mergers are important becomes evident by noting that they are around an order of magnitude more frequent than major mergers. Once the bulge mass reaches roughly M_C the ratio M_q/M_{bul} is around the average value inferred from the overall distribution at that redshift. Subsequently the mergers, minor as well as major, only create a small scatter around this value, consistent with the assumption of bulge-dominated mergers.

The trajectory in Fig. 7 suggests that the mean value of the conditional distribution will change with time, in co-evolution with the merger activity. Fig. 8 compares the mean value of M_q/M_{bul} found in the conditional distributions $p(M_q/M_{bul}|M_*)$ in five different redshift bins. At earlier times, the means show systematic lower fractions of quiescent components in their spheroids. This is connected to the higher fraction of available gas in major mergers at earlier times as can be seen in Fig. 9. The different averages show similar behaviours with stellar mass below M_C only differing by constant offsets and a slightly steeper increase of M_q/M_{bul} toward M_C . Above M_C , the starburst component in spheroids starts to increase again by up to $\sim 30\%$ depending on the redshift, a result of massive galaxies at high redshift likely being formed in a very gas-rich merger event, or having bulges that were formed very early on. At this point, it is not clear if this trend at high redshifts is real or just a product of not including feedback from super-massive black holes during major mergers and we will defer discussion of possible effects of AGN-feedback to a following paper (Khochfar & Silk in prep.). However, note that we usually do not find more than a few galaxies in the highest mass bins, which makes finding such galaxies very unlikely. From the different curves in Fig. 8, it is not obvious whether M_C plays the same fundamental role at all redshifts or if the characteristic mass scale changes with redshift. In any case,

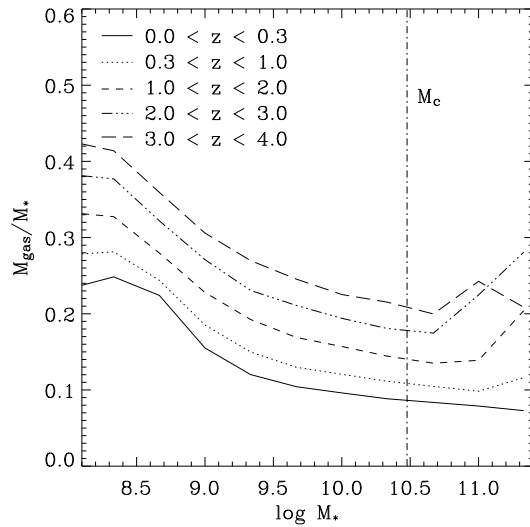


Figure 9. The evolution of the mean gas fraction in progenitors of major mergers as a function of stellar mass M_* in five different redshift bins between $z = 0$ and $z = 4$. Please note that M_* is the stellar mass of the merger remnant.

the differences according to our simulations are not very large for the overall galaxy population.

To understand the shape of the curves in Fig. 8 it is important to understand the extent to which the evolution in M_q/M_{bul} at each redshift and mass scale is driven by galaxies with different morphologies. In Fig. 10 we compare the overall stellar mass in spheroids divided by the total stellar mass present at different redshifts and masses. The closer to $M_{bul}/M_* = 1$, the more likely it is that most of the galaxies at a given mass scale are elliptical galaxies which have recently formed and did not regrow significantly large discs since then. At each redshift, our model predicts that the most massive galaxies, which are less massive with increasing redshift, are recently formed elliptical galaxies. As a consequence, the quiescent component in these galaxies resembles the average composition that results from major mergers at this redshift. Going to smaller galaxies, the bulge mass fractions decrease, indicating that more mass is found in stellar discs, which in turn means that the bulges must have formed earlier to allow for the growth of large stellar discs. As argued above, early mergers are more gas-rich and therefore lead to smaller ratios of M_q/M_{bul} . This, and the fact that galaxies with increasing mass have a larger number of minor mergers, which in general increase the quiescent component of bulges, accounts for the increase in the quiescent component in spheroids with increasing mass.

It is interesting to note that Fig. 10 suggests that the characteristic mass scale M_C approximately marks the transition point at which most of the stars start to be in spheroids independent of the redshift. Below M_C , the average distribution of stars in bulges and discs is roughly independent of the redshift, and shows the same mass dependence. Only at galaxy masses above M_C does the distribution of stars in spheroids and discs become significantly redshift-dependent. This behaviour can be attributed to two features of the CDM paradigm: first, the decline in the

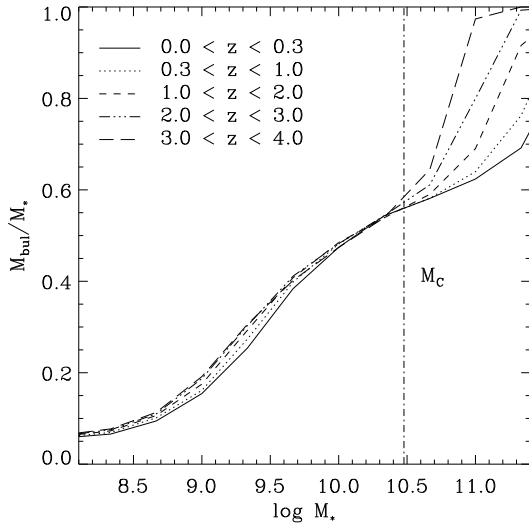


Figure 10. Bulge to total stellar mass fraction in five different redshift bins between $z = 0$ and $z = 4$. We calculated the fraction by summing up all stars present in spheroids at a given redshift and mass scale and dividing this value by the total amount of stars available at this mass scale. The vertical dot-dashed line marks the characteristic mass scale M_C .

merger rate going to lower redshifts and the connected ability of stellar discs to grow longer without being disrupted, and second, most massive galaxies at a given redshift are likely to be those which formed in a major merger, resulting in an elliptical galaxy.

To summarise, the build up of bulges and elliptical galaxies in a merger-driven model suggests that early gas-rich mergers lead to progenitors with a high fraction of stars in their spheroids, and which were formed during a dissipative central starburst event. This fraction is significantly higher than that found at later times in spheroids. While the progenitors of a present-day galaxy continue to grow stellar discs, minor mergers occur. These events tend to increase the quiescent fraction of stars in spheroids by contributing their disc stars to the spheroid of the remnant. These minor mergers occur mainly during the peak times in the merger activity which is dependent on the environment that the galaxy resides in (Khochfar & Burkert 2001). As soon as the bulge mass of the progenitor galaxies reaches $\sim M_C$, only small changes occur. However, depending on the morphology of the resultant galaxy the final stages might differ as well as the characteristic mass scale (Khochfar & Silk, in preparation).

4.2 Environmental Dependence

In paragraph 4.1 we presented the evolution of each individual stellar component in spheroids. This evolution is very dependent on the merger activity that galaxies experienced in their past. It is to be expected that the different evolutions of the merger rates with redshift in field and high density environments leave a characteristic signature in the merger component of spheroids.

In Fig. 11, we compare the fraction of quiescent com-

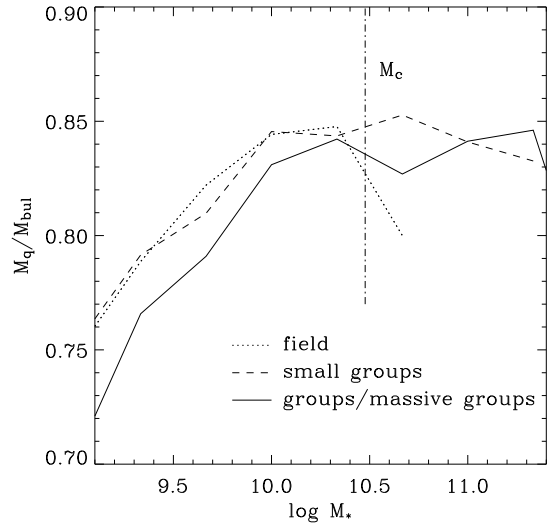


Figure 11. The evolution of the mean value M_q/M_{bul} of the conditional distribution $p(M_q/M_{bul}|M_*)$ as a function of stellar mass M_* in three different environments. We defined environments by the mass of the dark halo the galaxies reside in. Halos with $10^{12} M_\odot$, $10^{13} M_\odot$ and $10^{14} M_\odot$ are classified as field, small group and group/massive group environments, respectively.

ponents in the spheroids of galaxies found in different environments in our simulation. We classify environments into three different categories according to the mass of the dark matter halo the galaxies reside in. Galaxies in dark matter halos of $10^{12} M_\odot$, $10^{13} M_\odot$ and $10^{14} M_\odot$ are classified as field, small group, and group/massive group environments in our simulation. The average fraction of quiescent components in the bulges of spheroids less massive than $\sim M_C$ is systematically higher in field environments meaning their merger components are smaller. Furthermore we find in our simulations that there is no systematic difference for galaxies above $\sim M_C$. The difference between environments diminishes, the closer the galaxy mass is to M_C . Recalling the results of section 4.1, it becomes clear that massive galaxies in different environments are unaffected because the continuous growing by mergers, minor as well as major, erases the memory of the first merger epoch in different environments. Only those galaxies significantly less massive than $\sim M_C$ did not grow by many mergers after their initial mergers, but survived until today without much interactions as satellite galaxies. Since the initial merger is very much environmental dependent, gas-rich early mergers in high density environments and less gas-rich late mergers in field environments, differences arise between environments.

5 DISCUSSION AND CONCLUSION

In this paper we have investigated the origin of stars ending up in bulges and elliptical galaxies for systematic trends with mass, redshift and time of the last major merger. We divide stars in spheroids into two categories, merger and quiescent, according to their formation mode.

The merger component is associated with major merg-

ers in which cold gas in progenitor discs is driven to the centre of the remnant and a central starburst is ignited. Our simulations predict that the fraction of the merger component in spheroids is an increasing function of formation redshift and a decreasing function of spheroid mass. The latter is due to the longer time that progenitors of massive galaxies have to grow discs, and an enhanced number of minor mergers, which generally decreases the fraction. The higher fraction at earlier formation times is a result of the short cooling time scales for gas and the insufficient build up of stellar discs before the final major merger. Our simulations predict that the average merger component in the local galaxy population can be as high as 30% of the bulge mass in galaxies with $M_* \sim 10^9 M_\odot$ and as low as 15% in galaxies with $M_* > M_C = 3 \times 10^{10} M_\odot$.

The quiescent component is associated with stars previously formed in gaseous discs according to the Schmidt-Kennicutt law and later being added to the spheroid during major mergers. We find that the fraction of quiescent stars dominates bulges and elliptical galaxies. For galaxies above the critical mass scale, the fraction of quiescent stars becomes constant at a value of $M_q/M_{bul} \sim 85\%$, the result of mergers, minor as well as major, only introducing small deviations as soon as galaxies are more massive than M_C .

The fraction of stars in bulges and discs shows a remarkable relation with the galaxy mass scale. At galaxy masses below M_C , we find only a weak redshift dependency and a decreasing fraction of stars in bulges with decreasing mass. However, at masses above M_C we find a strong redshift dependence. At higher redshifts, the fraction of stars in bulges becomes larger in massive galaxies. This means that the most massive galaxies around at each redshift are likely to be elliptical galaxies and that only at later times do massive spiral galaxies start occurring.

Furthermore, our simulations indicate that mergers leading to remnants with mass larger than M_C always include progenitors with bulges and that more than 50% of the mass in progenitors of mass $M_* \sim M_C$ is in bulges. This has an important influence on the role of AGN-feedback as these bulges will harbour super-massive black holes.

Looking at the environmental dependence, we find that only galaxies less massive than M_C show differences. This is mainly related to the different epoch at which these galaxies assembled. Assembly is faster in high density environments resulting in larger merger components in bulges. Galaxies above M_C do not show any significant environmental dependency because of continued merger activity in contrast to smaller galaxies.

Recently Springel & Hernquist (2005) suggested that mergers between extremely gas-rich discs could lead to the formation of a disc galaxy during a major merger. The authors argued that these kind of mergers are likely to occur at high redshifts. However, our simulations indicate that the maximum gas fraction is at $\sim 40\%$ in mergers at high redshift and most likely between 20% – 30% for a wide range of masses and redshifts. In general the gas fraction in mergers is a decreasing function of mass. At very large masses and at high redshifts a small population of gas rich massive mergers occurs, which tends to slightly deviate from this trend. A reason for these events in our simulation could be associated with missing feedback from AGNs. Those massive gas-rich

mergers at high redshift are likely to have progenitors with black holes.

Simulations by Springel & Hernquist (2005) show that in general the merger component is more centrally concentrated than the quiescent component. The effective radius of the merger component in their simulation is ~ 5.7 times smaller than that of the quiescent component. This suggests an interesting behaviour for the sizes of two galaxies of the same mass but different merger component. The remnant from the merger including less gas and hence less merger component will have a larger size. As we have shown above remnants at higher redshifts have larger merger fractions. This and the observational indication that disc galaxies at higher redshifts are smaller (e.g. Trujillo et al. 2005) might be able to account for the observed size-evolution of elliptical galaxies (Daddi et al. 2005; Trujillo et al. 2005).

We would like to thank Ignacio Trujillo and Emanuele Daddi for pointing out the high redshift data. SK acknowledges funding by the PPARC Theoretical Cosmology Rolling Grant.

REFERENCES

- Barnes, J. E. 2001, Astronomical Society of the Pacific Conference Series, 240, 135
- Barnes, J. E. 2002, MNRAS, 333, 481
- Barnes, J. E., & Hernquist, L. E. 1991, ApJL, 370, L65
- Barnes, J. E. & Hernquist, L. 1992, Ann. Rev. of Astronomy and Astrophysics, 30, 705
- Barnes, J. E. 1998, Saas-Fee Advanced Course 26: Galaxies: Interactions and Induced Star Formation, 275
- Bell, E., et al. 2005, astro-ph/0506425
- Bender, R., Burstein, D., & Faber, S. M. 1993, ApJ, 411, 153
- Benson, A. J., Lacey, C. G., Baugh, C. M., Cole, S., & Frenk, C. S. 2002, MNRAS, 333, 156
- Benson, A. J., Bower, R. G., Frenk, C. S., Lacey, C. G., Baugh, C. M., & Cole, S. 2003, ApJ, 599, 38
- Burkert, A & Naab, T. 2003, in Galaxies and Chaos, eds. G. Contopoulos, N. Voglis, Lecture Notes in Physics, 626, p327
- Cimatti, A., et al. 2004, Nature, 430, 184
- Cole, S., Aragon-Salamanca, A., Frenk, C. S., Navarro, J. F., & Zepf, S. E. 1994, MNRAS, 271, 781
- Cole, S., Lacey, C. G., Baugh, C. M., & Frenk, C. S. 2000, MNRAS, 319, 168
- Cole, S., et al. 2001, MNRAS, 326, 255
- Cox, T. J., Jonsson, P., Primack, J. R., Somerville, R. S., astro-ph/0503201
- Croton, D. J., et al. 2006, MNRAS, 365, 11
- Daddi, E., et al. 2005, ApJ, 626, 680
- van Dokkum, P. G. 2005 astro-ph/0506661 (AJ accepted for pub.)
- Giovanelli, R., Haynes, M. P., da Costa, L. N., Freudling, W., Salzer, J. J., & Wegner, G. 1997, ApJL, 477, L1
- Gnedin, N. Y. 2000, ApJ, 542, 535
- Haehnelt, M. G. & Kauffmann, G. 2000, MNRAS, 318, L35
- Huang, J.-S., Glazebrook, K., Cowie, L. L., & Tinney, C. 2003, ApJ, 584, 203
- Jenkins, A., Frenk, C. S., White, S. D. M., Colberg, J. M.,

- Cole, S., Evrard, A. E., Couchman, H. M. P., & Yoshida, N. 2001, MNRAS, 321, 372
- Kauffmann, G., Colberg, J. M., Diaferio, A., & White, S. D. M. 1999, MNRAS, 303, 188 (K99)
- Kauffmann, G., & Haehnelt, M. 2000, MNRAS, 311, 576
- Kauffmann, G., et al. 2003, MNRAS, 341, 54
- Kauffmann, G., et al. 2004, MNRAS, 353, 713
- Kennicutt, R. C. 1998, ApJ, 498, 541
- Khochfar, S. & Burkert, A. 2001, ApJ, 561, 517
- Khochfar, S. & Burkert, A. 2003, ApJL, 597, L117
- Khochfar, S., & Burkert, A. 2006, A & A, 445, 403
- Khochfar, S., & Burkert, A. 2005, MNRAS, 359, 1379
- Kochanek, C. S., et al. 2001, ApJ, 560, 566
- Chiosi, C., & Carraro, G. 2002, MNRAS, 335, 335
- Kogut, A., et al. 2003, ApJS, 148, 161
- Larson, R. B. 1974, MNRAS, 166, 585
- Lauer, T. R., et al. 1995, AJ, 110, 2622
- McDermid, R. M., et al. 2005, astro-ph/0508631
- Mihos, J. C., & Hernquist, L. 1996, ApJ, 464, 641
- Naab, T., & Burkert, A. 2003, ApJ, 597, 893
- Navarro, J. F., & Steinmetz, M. 1997, ApJ, 478, 13
- Scalo, J. M. 1986, Fundamentals of Cosmic Physics, 11, 1
- Schweizer, F. 2005, ASSL Vol. 329: Starbursts: From 30 Doradus to Lyman Break Galaxies, 143
- Shen, S., Mo, H. J., White, S. D. M., Blanton, M. R., Kauffmann, G., Voges, W., Brinkmann, J., & Csabai, I. 2003, MNRAS, 343, 978
- Simien, F., & de Vaucouleurs, G. 1986, ApJ, 302, 564
- Silk, J. 1977, ApJ, 211, 638
- Somerville, R. S. & Kolatt, T. S. 1999, MNRAS, 305, 1
- Somerville, R. S., & Primack, J. R. 1999, MNRAS, 310, 1087
- Somerville, R. S., Lemson, G., Kolatt, T. S., & Dekel, A. 2000, MNRAS, 316, 479
- Somerville, R. S. 2002, ApJL, 572, L23
- Spergel, D. N., et al. 2003, ApJS, 148, 175
- Springel, V., & Hernquist, L. 2005, ApJL, 622, L9
- Springel, V., White, S. D. M., Tormen, G., & Kauffmann, G. 2001, MNRAS, 328, 726 (S01)
- Sutherland, R. S., & Dopita, M. A. 1993, ApJS, 88, 253
- Thomas, D., Maraston, C., Bender, R., & de Oliveira, C. M. 2005, ApJ, 621, 673
- Toomre, A. & Toomre, J. 1972, ApJ, 178, 623
- Trujillo, I., et. al, astro-ph/0504225
- White, S. D. M. & Frenk, C. S. 1991, ApJ, 379, 52
- White, S. D. M., & Rees, M. J. 1978, MNRAS, 183, 341